



## Short communication

Effects of magnesium doping on electronic conductivity and electrochemical properties of  $\text{LiFePO}_4$  prepared via hydrothermal route

Xiuqin Ou\*, Guangchuan Liang, Li Wang, Shengzhao Xu, Xia Zhao

Institute of Power Source &amp; Ecomaterials Science, Box 1055, Hebei University of Technology, Tianjin 300130, China

## ARTICLE INFO

## Article history:

Received 22 December 2007

Received in revised form 21 February 2008

Accepted 22 February 2008

Available online 4 March 2008

## Keywords:

Lithium iron phosphate

Magnesium

Doping

Electronic conductivity

Hydrothermal synthesis

## ABSTRACT

Carbon free composites  $\text{Li}_{1-x}\text{Mg}_x\text{FePO}_4$  ( $x=0.00, 0.02$ ) were synthesized from  $\text{LiOH}$ ,  $\text{H}_3\text{PO}_4$ ,  $\text{FeSO}_4$  and  $\text{MgSO}_4$  through hydrothermal route at  $180^\circ\text{C}$  for 6h followed by being fired at  $750^\circ\text{C}$  for 6 h. The samples were characterized by X-ray diffraction (XRD), high-resolution transmission electron microscopy (HRTEM), flame atomic absorption spectroscopy and electronic conductivity measurement. To investigate their electrochemical properties, the samples were mixed with glucose as carbon precursors, and fired at  $750^\circ\text{C}$  for 6 h. The charge–discharge curves and cycle life test were carried out at  $23 \pm 2^\circ\text{C}$ . The Rietveld refinement results of lattice parameters of the samples indicate that the magnesium ion has been successfully doped into the M1 (Li) site of the phospho-olivine structure. With the same order of magnitude, there is no material difference in terms of the electronic conductivities between the doped and undoped composites. Conductivities of the doped and undoped samples are  $10^{-10} \text{ S cm}^{-1}$  before being fired,  $10^{-9} \text{ S cm}^{-1}$  after being fired at  $750^\circ\text{C}$ , and  $10^{-1} \text{ S cm}^{-1}$  after coated with carbon, respectively. Both the doped and undoped composites coated with carbon exhibit comparable specific capacities of  $146 \text{ mAh g}^{-1}$  vs.  $144 \text{ mAh g}^{-1}$  at  $0.2 \text{ C}$ ,  $140 \text{ mAh g}^{-1}$  vs.  $138 \text{ mAh g}^{-1}$  at  $1 \text{ C}$ , and  $124 \text{ mAh g}^{-1}$  vs.  $123 \text{ mAh g}^{-1}$  at  $5 \text{ C}$ , respectively. The capacity retention rates of both doped and undoped samples over 50 cycles at  $5 \text{ C}$  are close to 100% (vs. the first-cycle corresponding C-rate capacity). Magnesium doping has little effects on electronic conductivity and electrochemical properties of  $\text{LiFePO}_4$  composites prepared via hydrothermal route.

© 2008 Elsevier B.V. All rights reserved.

## 1. Introduction

Lithium iron phosphate has been recognized as a promising candidate to replace lithium cobalt oxide as the cathode material of Li-ion batteries, which is now attracting commercial interests due to such advantages as possibly lower cost, improved safety, and highly reversible and repeatable property. However, the low ionic and electronic conductivity has greatly inhibited its high-rate applications [1]. Efforts to increase conductivity of electrode made from  $\text{LiFePO}_4$  have focused on particle size reducing [2–5], intimate conducting phase coating [6–9], and metals supervalent doping [10–17]. The mechanism and effect of coating on the particles to enhance the electronic conductivity and reducing the particle size to overcome the weak ionic conductivity have been widely approved. However, the mechanism and effect of supervalent cation doping on electronic conductivity reported so far are still in controversy. The mechanism and positive effect of supervalent cation doping on conductivity of  $\text{LiFePO}_4$  were firstly suggested by Chiang et al. [10] in 2002, and then questioned by Herle et al.

[11] in 2004, which has attracted much attention. Chiang et al. [10] and others [12–20] hold that the improvement of electronic conductivity is due to the fact that the ion dopant mainly takes the site of Li (M1), leading to the co-existence of  $\text{Fe}^{2+}$  and  $\text{Fe}^{3+}$  in single phase. It is well known that trace amount of  $\text{Fe}^{3+}$  can be detected easily by thiocyanate colorimetric method. Unfortunately, all the reports offered little adequate evidence to prove that the  $\text{Fe}^{3+}$  content increases after supervalent cation doping. Moreover, the results showed the improvement of electronic conductivity to varying degrees. For example, Chiang et al. [10] reported an increase by 8 orders of magnitude in the electronic conductivity of the cation doped olivine-type materials  $\text{Li}_{1-x}\text{M}_x\text{FePO}_4$  ( $\text{M} = \text{Nb}, \text{Mg}, \text{Al}, \text{Ti}, \text{W}$ , etc.) regardless of the valence and radius of the ion. Whereas, Zhou et al. [13] reported that the effect of cation ( $\text{Mg}$ ,  $\text{Sm}$ ,  $\text{Zr}$  and  $\text{Nb}$ ) doping on electronic conductivity relates not only to ion radius but also to valence.  $\text{LiFePO}_4$  doped with ions with smaller radius and higher valence showed better electrochemical characters. They also synthesized  $\text{Li}_{1-x}\text{M}_x\text{FePO}_4$  ( $\text{M} = \text{Mg}, \text{Cu}$  and  $\text{Zn}$ ), whose conductivity increased 3 orders of magnitude [16]. Yuan et al. [17] reported that the conductivity of  $\text{Li}_{0.99}\text{Mo}_{0.01}\text{FePO}_4$  is greater than that of the undoped sample by 2 orders of magnitude. Chen et al. [19] carried out a series of theoretical and experimental research in  $\text{Cr}^{3+}$  ion doped  $\text{LiFePO}_4$ . These various results cannot support the argument

\* Corresponding author. Tel.: +86 22 60202406; fax: +86 22 26564850.  
E-mail address: [ouxuqin@hebut.edu.cn](mailto:ouxuqin@hebut.edu.cn) (X. Ou).

put forward by Chiang et al. [10]. The interpretation of the increase of intrinsic electronic conductivity was suspected by Herle et al. [11], who synthesized the Zr-containing composite using identical method to Chiang's [10]. They hold that the conducting phases (iron phosphides and/or phosphocarbides), not carbon, is primarily responsible for the increase of electronic conductivity, due to Li-deficient  $\text{LiFePO}_4$  reduction at the surface of the particles, rather than a mixed-valent metal  $\text{M}^{2+/3+}$  in single phase. Similar views have been reported. For example, Masquelier et al. [21] reported that the doping of Nb in  $\text{LiFePO}_4$  lead to the formation of crystalline  $\beta\text{-NbPO}_4$  and/or an amorphous (Nb, Fe, C, O and P) 'cobweb' around  $\text{LiFePO}_4$ , which is responsible for superior electrochemical activity, rather than the formation of crystalline  $\text{Li}_{1-x}\text{Nb}_x\text{FePO}_4$ . The electronic conductivity of pure  $\text{LiFePO}_4$  and  $\text{LiFePO}_4/\beta\text{-NbPO}_4$  composites was  $\sim 10^{-9} \text{ S cm}^{-1}$  while that of Nb- and/or C-containing  $\text{LiFePO}_4$  composites increased up to  $1.6 \times 10^{-1} \text{ S cm}^{-1}$ . Franger et al. [22] synthesized the  $\text{LiFePO}_4$  composite using  $\text{Li}_3\text{PO}_4$  and fresh iron phosphate as the source of the main components and sucrose and boron phosphate as the source of electronic conductor precursor. Electrochemical results indicated that the specific capacity is less sensitive to an increase of the discharge rate in the case of boron composite  $\text{LiFePO}_4$ . The enhancement of the electronic conductivity and the noticeable improvement of the lithium ionic diffusion into the host lattice are responsible for the formation of a highly conductive boron-based wrap around the particles. Yang et al. [23] synthesized  $\text{LiFePO}_4$ -based powders with vanadium addition using solution method. The sample obtained was composed of well-mixed  $\text{LiFePO}_4$  and  $\text{Li}_3\text{V}_2(\text{PO}_4)_3$  phases instead of doped material in a single phase.

The cause leading to the various results cited above is related to the preparation process. The researchers referred to above obtained their samples mostly from the solid-state reaction at high temperature using ferrous oxalate as raw material and alkoxide as dopant. Small amounts of carbon contaminant that invariably result from both the oxalate precursor and the alkoxide in the metal dopant have been considered as a contributing factor to conductivity, and therefore, factors based on sources of carbon are suspicious. Moreover, metal phosphates have a propensity to undergo carbothermal reduction at high temperature, leading to the formation of conducting nanophases, which in turn interferes with the effects of supervalent cation doping on electronic conductivity and electrochemical properties.

In order to clarify the effect of supervalent cation doping on  $\text{LiFePO}_4$  composites, the hydrothermal method was applied to prepare  $\text{LiFePO}_4$ , which is believed to be a useful method for preparing fine particles. This method has been chosen for two additional advantages: the products are formed at low temperature, and the precursors contain no organic reactant. This method can also avoid the effects of carbon residue resulting from organic precursor decomposition and those of subsidiary products resulting from the carbothermal reaction at high temperature.

## 2. Experimental

$\text{LiFePO}_4$  doped with magnesium was prepared through a hydrothermal process in a 10 L stainless steel autoclave (Weihai Co., China, Model WHF-10L). Starting materials were  $\text{LiOH}\cdot\text{H}_2\text{O}$  (purity > 99.5 wt%),  $\text{FeSO}_4\cdot 7\text{H}_2\text{O}$  (purity > 99.5 wt%),  $\text{H}_3\text{PO}_4$  (*o*- $\text{H}_3\text{PO}_4$ , 85 wt%), and  $\text{MgSO}_4\cdot 7\text{H}_2\text{O}$  (purity > 99.5 wt%). The molar ratio of Li:Fe:P:Mg in the precursor solution was 3:0.98:1:*x* (*x*=0.00, 0.02), the concentration of  $\text{Fe}^{2+}$  in the reaction solution was controlled to be  $0.5 \text{ mol L}^{-1}$ .  $\text{LiOH}\cdot\text{H}_2\text{O}$ ,  $\text{FeSO}_4\cdot 7\text{H}_2\text{O}$  and  $\text{MgSO}_4\cdot 7\text{H}_2\text{O}$  were dissolved in deionized water separately.  $\text{LiOH}$  solution,  $\text{H}_3\text{PO}_4$  solution were mixed in autoclave, then  $\text{FeSO}_4$  solution and  $\text{MgSO}_4$  solution were added subsequently. All the

operation processes were carried out under the protection of  $\text{N}_2$  atmosphere. The autoclave was sealed and heated at  $180^\circ\text{C}$  for 6 h. Afterwards, the solution was cooled down to room temperature. The precipitate was filtered and washed several times with deionized water. The filter cake was dried at  $120^\circ\text{C}$  for 12 h in a vacuum oven. The dried sample was fired at  $750^\circ\text{C}$  for 6 h under a  $\text{N}_2$  atmosphere. In order to evaluate the electrochemical properties of  $\text{LiFePO}_4$ ,  $\text{LiFePO}_4/\text{C}$  composite was prepared by firing  $\text{LiFePO}_4$  with glucose ( $\text{LiFePO}_4$ :glucose = 1:0.3, w/w) under the same conditions.

The crystallographic structure of the samples was characterized by an X-ray diffractometer (Rigaku D/max 2500 V/PC) with a  $\text{Cu K}\alpha$  radiation source ( $\lambda = 0.15406 \text{ nm}$ ). The diffraction data were collected for 2 s at each  $0.02^\circ$  step width over a  $2\theta$  range from  $20^\circ$  to  $70^\circ$ . Lattice parameters for the lithium iron phosphate were refined by Rietveld analysis using Rietica 1.77 software. The morphology and the surface texture of crystal were observed by high-resolution transmission electron microscopy (HRTEM) (Philips, Tecnai F20) operated at 200 kV accelerating voltage. Magnesium composition of the samples was determined by flame atomic absorption spectrometry (Thermo-m6). Ferric iron ( $\text{Fe}^{3+}$ ) content was detected by ferric thiocyanate colorimetric method. 0.01 g  $\text{LiFePO}_4$  powder was dissolved in 5 mL 10 wt% hydrochloride acid solution, and 1 mL 20% ammonium thiocyanate solution was added, then the solution was diluted to 50 mL. Meanwhile, a series of ferric iron colorimetric standard solution resulted from the same procedures. The results were obtained from comparing the color of the sample with those of ferric iron colorimetric standard solution. To measure the electronic conductivity, the powder was pressed to disc-shaped pellet at the pressure of 50 MPa. The conductivity was measured by two-point dc method using a Model J0410 Multimeter (Hangzhou, China). The electrochemical performance of  $\text{LiFePO}_4$  samples was tested using a coin-type cell (size: 2430). The composite electrode was prepared by mixing  $\text{LiFePO}_4$ , carbon (super P-MMM Carbon) conductive additive and polytetrafluoroethylene (PTFE) in a weight ratio of 8:1:1. These film-type  $\text{LiFePO}_4$  electrodes were assembled in coin cells with lithium metal as a counter electrode separated by a Celgard 2400 separator. The electrolyte was a mixed solvent of ethylene carbonate (EC), diethyl carbonate (DEC) and dimethyl carbonate (DMC) (1:1:1, v/v/v) containing  $1.0 \text{ mol L}^{-1}$   $\text{LiPF}_6$ . The cathode performance was investigated in terms of charge–discharge curves and cycling capacity using an automatic charge–discharge instrument (Model CT2001A Land Co., China,) in the cut-off voltages of 2.3 and 4.2 V. All the electrochemical measurements were carried out at ambient temperature ( $23 \pm 2^\circ\text{C}$ ).

## 3. Results and discussion

Magnesium composition analysis results show that the magnesium dopant has transferred completely into the product. Fig. 1 shows the X-ray diffraction (XRD) profiles of the  $\text{Li}_{1-x}\text{Mg}_x\text{FePO}_4$  (*x*=0.00, 0.02) samples. The XRD patterns of the samples agree very well with that of phospho-olivine  $\text{LiFePO}_4$  indexed with orthorhombic *Pnma* space group (No. 62), and no magnesium entity or other impurity phase was detected. Both samples have narrow diffraction peaks, which indicate a good crystallinity degree. Table 1 lists the Rietveld refined lattice parameters of  $\text{LiFePO}_4$  and  $\text{Li}_{0.98}\text{Mg}_{0.02}\text{FePO}_4$ . The results show that magnesium dopant has been successfully doped into the Li (M1) site without affecting the phospho-olivine structure. Low concentration magnesium doping leads to the shrinkage of crystal cell due to the smaller radius of  $\text{Mg}^{2+}$  ion (0.066 nm) than that of  $\text{Li}^+$  ion (0.076 nm) [13]. Additionally, the  $\text{Fe}^{3+}$  contents of unfired samples of both the doped and the undoped are 0.5 wt% and those of carbon coated samples of both the doped and the undoped are 0.4 wt%, which indicates that  $\text{Fe}^{3+}$

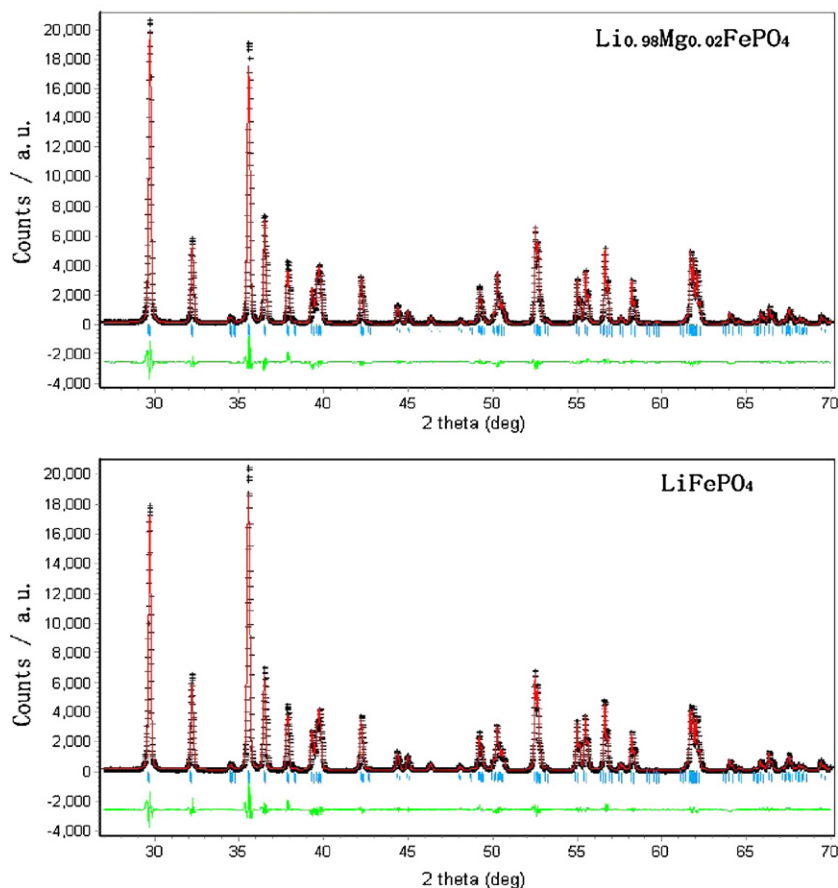


**Fig. 1.** X-ray powder diffraction patterns of magnesium doped and undoped  $\text{LiFePO}_4$  samples, hydrothermally synthesized at  $180^\circ\text{C}$  for 6 h and fired at  $750^\circ\text{C}$  for 6 h in pure  $\text{N}_2$ .

content is not affected by magnesium doping, but is reduced by carbon coating during the carbon coating process regardless of doped or undoped samples.

The electronic conductivities of the undoped and doped compounds are shown in Table 2. With the same order of magnitude,

**Table 1**

Cell parameters of  $\text{LiFePO}_4$  and  $\text{Li}_{0.98}\text{Mg}_{0.02}\text{FePO}_4$  synthesized through hydrothermal route followed by being fired at  $750^\circ\text{C}$

	Formula	
	$\text{LiFePO}_4$	$\text{Li}_{0.98}\text{Mg}_{0.02}\text{FePO}_4$
Space group	<i>Pnma</i> (No. 62)	<i>Pnma</i> (No. 62)
Lattice parameters		
<i>a</i> (nm)	1.03221	1.03197
<i>b</i> (nm)	0.60039	0.60024
<i>c</i> (nm)	0.46904	0.46902
Unit cell volume ( $\text{nm}^3$ )	0.29068	0.29052
Formula units per unit cell	4	4
$R_p$	0.06421	0.06457
$R_{wp}$	0.08644	0.08605
$\chi^2$	0.05094	0.05152

**Table 2**

Electronic conductivities of prepared samples ( $\sigma$ ,  $\text{S cm}^{-1}$ )

	Samples	
	$\text{LiFePO}_4$	$\text{Li}_{0.98}\text{Mg}_{0.02}\text{FePO}_4$
Before fired	$10 \times 10^{-10}$	$6.2 \times 10^{-10}$
Fired at $750^\circ\text{C}$	$3.7 \times 10^{-9}$	$3.8 \times 10^{-9}$
Coated with carbon	$2.0 \times 10^{-1}$	$1.9 \times 10^{-1}$

there is no material difference between the doped and the undoped in terms of electronic conductivity. The conductivities are  $10^{-10} \text{ S cm}^{-1}$  before being fired,  $10^{-9} \text{ S cm}^{-1}$  after being fired at  $750^\circ\text{C}$ , and  $10^{-1} \text{ S cm}^{-1}$  after being coated with carbon, respectively. The small numerical discrepancy is attributable to the measurement error. The conductivity of the fired samples (carbon free) is greater than that of the unfired one by  $\sim 1$  order in magnitude, suggesting that the additional heat treatment increases the conductivity of hydrothermally synthesized  $\text{LiFePO}_4$  probably due to the crystallization of amorphous phase on the surface of the particle, which can be confirmed by TEM images in Fig. 2. From Fig. 2, it can be seen that there is a very thin film on the surface of the grains, which is less than 1 nm and considered as amorphous phase. The surface become smooth, accompanying the disappearance of amorphous film after the sample was fired at  $750^\circ\text{C}$ . On the basis of conductivities measurements, it can be concluded that magnesium doping has little effect on the improvement of electronic conductivity. On the other hand, it can also be observed from Fig. 2 that the powders are composed of slightly agglomerated particles, and the primary particles show flat shape and the grain dimensions of  $0.5\text{--}1 \mu\text{m}$  in edge and about  $0.1 \mu\text{m}$  in thickness.

The electrochemical performances of the samples are shown in Figs. 3 and 4. Fig. 3 shows the second cycle of voltage profile of the doped and undoped  $\text{LiFePO}_4/\text{C}$  composites. In the case of 5 C discharge, the electrode was charged at 1 C rate. Both samples have similar charge–discharge curves with flat plateaus corresponding to the lithium deintercalation and intercalation. In the case of 0.2 C, the charge voltage plateau is 3.46 V for both  $\text{Li}_{0.98}\text{Mg}_{0.02}\text{FePO}_4/\text{C}$  and  $\text{LiFePO}_4/\text{C}$ , while the discharge voltage plateau is 3.40 V for

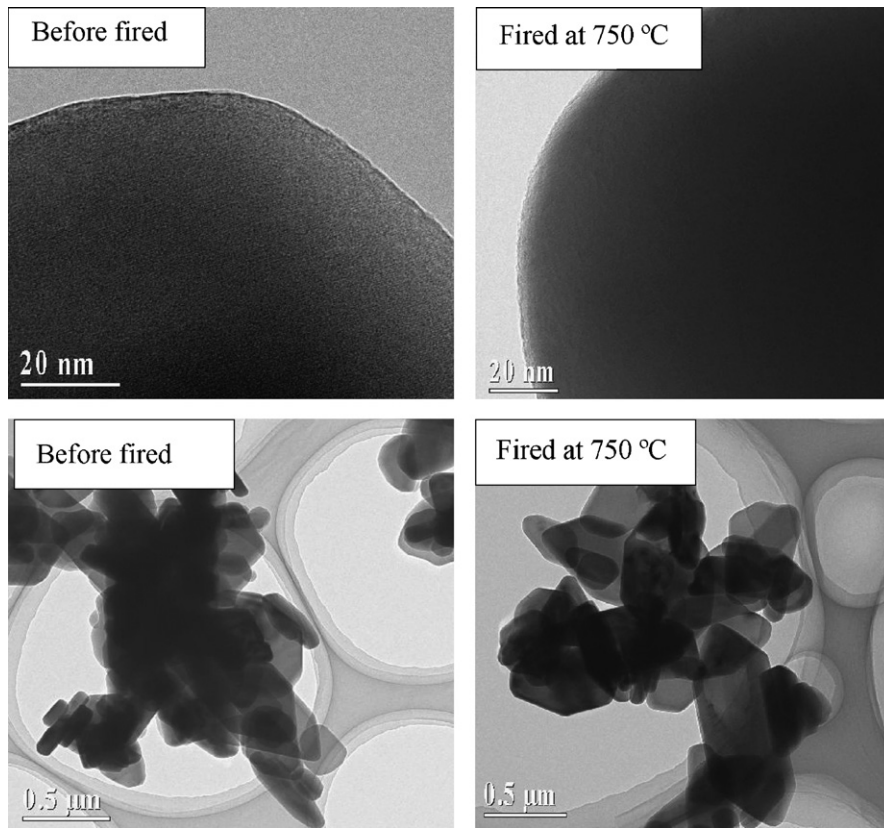


Fig. 2. TEM images of  $\text{LiFePO}_4$  particles before and after fired at  $750^\circ\text{C}$  in pure  $\text{N}_2$ .

$\text{Li}_{0.98}\text{Mg}_{0.02}\text{FePO}_4/\text{C}$  and  $3.39\text{V}$  for  $\text{LiFePO}_4/\text{C}$ . The potential intervals are  $0.06$  and  $0.07\text{V}$  for  $\text{Li}_{0.98}\text{Mg}_{0.02}\text{FePO}_4/\text{C}$  and  $\text{LiFePO}_4/\text{C}$ , respectively. Both samples show a smaller value of potential interval compared with that which has been reported in references [13,16,20], which indicates the enhancement of electrode reaction reversibility. The specific discharge capacities of magnesium doped  $\text{Li}_{0.98}\text{Mg}_{0.02}\text{FePO}_4/\text{C}$  are  $146\text{mAh g}^{-1}$  at  $0.2\text{C}$  and  $124\text{mAh g}^{-1}$  at  $5\text{C}$ , and those of the undoped  $\text{LiFePO}_4/\text{C}$  are  $144\text{mAh g}^{-1}$  at  $0.2\text{C}$  and  $123\text{mAh g}^{-1}$  at  $5\text{C}$ , respectively, indicating that there is little difference in specific capacity between the doped sample and the undoped one.

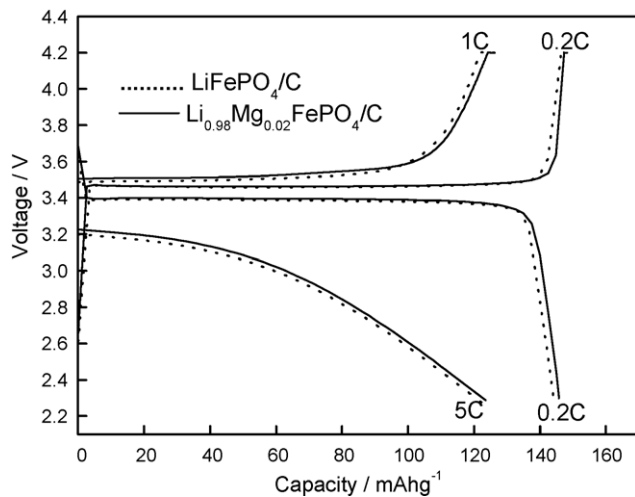


Fig. 3. Charge and discharge curves of  $\text{LiFePO}_4$  and  $\text{Li}_{0.98}\text{Mg}_{0.02}\text{FePO}_4$ . Current density =  $15\text{mAh g}^{-1}$ .

Fig. 4 shows the cycling behaviors of the doped and undoped  $\text{LiFePO}_4/\text{C}$  composites at room temperature. At the rates of  $0.2$ ,  $1$  and  $5\text{C}$ , the electrode was charged up to  $4.2\text{V}$  at  $0.2$ ,  $1$ ,  $1\text{C}$  and discharged at  $0.2$ ,  $1$ ,  $5\text{C}$  rates, respectively. The carbon coated composites of both the doped and the undoped show comparable specific discharge capacities of  $146\text{mAh g}^{-1}$  vs.  $144\text{mAh g}^{-1}$  at  $0.2\text{C}$ ,  $140\text{mAh g}^{-1}$  vs.  $138\text{mAh g}^{-1}$  at  $1\text{C}$ , and  $124\text{mAh g}^{-1}$  vs.  $123\text{mAh g}^{-1}$  at  $5\text{C}$ , respectively. The capacity retention rates over  $50$  cycles at  $5\text{C}$  are close to  $100\%$  (vs. the first corresponding C-rate capacity), which indicate the good cycling stability of the samples whether doped or not. The excellent electrochemical properties of specific discharge capacity, rate capability and cycling stability can be contributed to the thinnest flat shape of the crystal of the materials, and/or to the hydrothermal synthe-

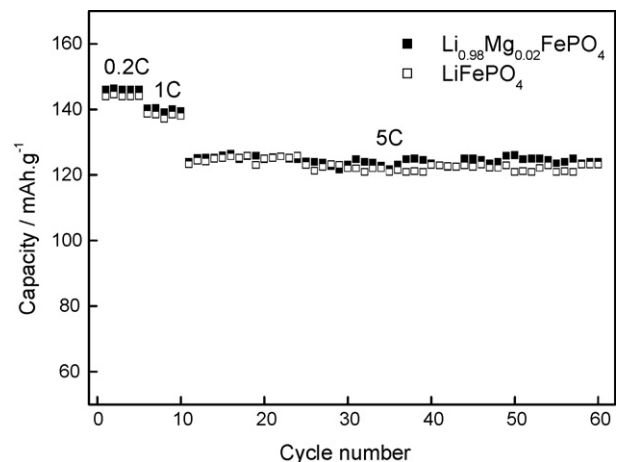


Fig. 4. Cycling performances of the doped and undoped  $\text{LiFePO}_4/\text{C}$ .

sis conditions under which nonstoichiometric LiFePO<sub>4</sub> is produced. Investigation of the mechanism on nonstoichiometric LiFePO<sub>4</sub> to obtain enhanced electrochemical properties will be reported in due course.

#### 4. Conclusion

Well-crystalline and pure phase lithium iron phosphate and its doped derivative have been successfully synthesized through hydrothermal route. The electronic conductivities of both the doped and undoped LiFePO<sub>4</sub> have no material difference. Both samples exhibit similar specific discharge capacities at various C-rates, and the capacity retention rates are very close to 100% over 50 cycles at 5 C at ambient temperature of 23 ± 2 °C. The excellent electrochemical properties of specific discharge capacity, rate capability and cycling stability could be contributed to the thinnest flat shape of the crystal of the materials, and/or to the hydrothermal synthesis conditions under which nonstoichiometric LiFePO<sub>4</sub> is produced. Magnesium doping has little effect on electronic conductivity and electrochemical properties of LiFePO<sub>4</sub> synthesized by hydrothermal route.

#### References

- [1] A.S. Anderesson, J.O. Thomas, *J. Power Sources* 97–98 (2001) 498.
- [2] H.S. Kim, B.W. Cho, W.I. Cho, *J. Power sources* 132 (2004) 235.
- [3] M.R. Yang, W.H. Ke, S.H. Wu, *J. Power Sources* 146 (2005) 539.
- [4] S.H. Wu, K.M. Hsiao, W.R. Liu, *J. Power Sources* 146 (2005) 550.
- [5] T.H. Cho, H.T. Chung, *J. Power Sources* 133 (2004) 272.
- [6] H. Huang, S.C. Yin, L.F. Nazar, *Electrochem. Solid-State Lett.* 4 (2001) A170.
- [7] K.S. Park, J.T. Son, H.T. Chung, S.J. Kim, C.H. Lee, K.T. Kang, H.G. Kim, *Solid State Commun.* 129 (2004) 311.
- [8] Z. Chen, J.R. Dahn, *J. Electrochem. Soc.* 149 (2002) A1184.
- [9] F. Crose, A.D. Epifanio, J. Hassoun, A. Deptula, T. Olczac, B. Scrosati, *Electrochem. Solid-State Lett.* 5 (2002) A47.
- [10] S.Y. Chung, J.T. Bloking, Y.M. Chiang, *Nat. Mater.* 1 (2002) 123.
- [11] P.S. Herle, B. Ellis, N. Coombs, L.F. Nazar, *Nat. Mater.* 3 (2004) 147.
- [12] J.R. Ying, M. Lei, C.Y. Jiang, C.R. Wan, X.M. He, J.J. Li, L. Wang, J.G. Ren, *J. Power Sources* 158 (2006) 543.
- [13] J.F. Ni, H.H. Zhou, J.T. Chen, X.X. Zhang, *Chin. J. Inorg. Chem.* 21 (2005) 472.
- [14] D. Wang, H. Li, S. Shi, X. Huang, L. Chen, *Electrochem. Acta* 50 (2005) 2955.
- [15] G.X. Wang, S.L. Bewlay, K. Konstantinov, H.K. Liu, S.X. Dou, J.-H. Ahn, *Electrochem. Acta* 50 (2004) 443.
- [16] J.F. Ni, H.H. Zhou, J.T. Chen, X.X. Zhang, *Mater. Lett.* 59 (2005) 2361.
- [17] M. Zhang, L.F. Jiao, H.T. Yuan, Y.M. Wang, J. Guo, M. Zhao, W. Wang, X.D. Zhou, *Solid State Ionics* 177 (2006) 3309.
- [18] H. Xie, Z.T. Zhou, *Electrochim. Acta* 51 (2006) 2063.
- [19] J.F. Ni, H.H. Zhou, J.T. Chen, G.Y. Su, *Acta Phys.-Chim. Sinica* 20 (2004) 582.
- [20] G.X. Wang, S.L. Bewlay, K. Konstantiov, H.K. Liu, S.X. Dou, J.-H. Ahn, *Electrochim. Acta* 50 (2004) 443.
- [21] C. Delacourt, C. Wurm, L. Laffont, J.B. Leriche, C. Masquelier, *Solid State Ionics* 177 (2006) 333.
- [22] S. Franger, C. Benoit, C. Bourbon, F. Le Cras, *J. Phys. Chem. Solids* 67 (2006) 1338.
- [23] M.R. Yang, W.H. Ke, S.H. Wu, *J. Power Sources* 165 (2007) 646.